THE ASTROPHYSICAL JOURNAL, 562:L91–L94, 2001 November 20

STAR FORMATION SIGNATURES IN THE CONDENSATION DOWNSTREAM OF HH 80N

J. M. GIRART,[1,2] R. ESTALELLA,[1] S. VITI,[3] D. A. WILLIAMS,[3] AND P. T. P. HO[4]

Received 2001 July 18; accepted 2001 October 10; published 2001 October 26

ABSTRACT

HH 80 North (hereafter HH 80N) is one of the Herbig-Haro objects associated with quiescent dense clumps. We report CO and CS BIMA observations that reveal star formation within the HH 80N dense clump. The CO emission clearly reveals a bipolar molecular outflow centered on the dense clump. The CS emission traces a ringlike structure of radius $\simeq$0.24 pc. The CS kinematics shows that the ring is collapsing with an infall speed of $\sim$0.6 km s^{-1}. The required mass to produce the collapse is in agreement with previous ammonia observations of the 20 $M_\odot$ core, which is embedded within the CS structure. However, we cannot discard that the ring structure, driven by protostellar winds, is expanding if the CS abundance is unusually high and if the CO momentum rate is much higher than that measured because of inclination and optical depth effects. The properties of the molecular outflow and of the dense core suggest that it harbors a Class 0 object. There are also signatures of the interaction of the HH 80/81/80N outflow with the dense gas. In particular, it is possible that the HH 80/81/80N outflow has triggered or at least sped up the star formation in this region.

Subject headings: ISM: individual (HH 80 North) — ISM: jets and outflows — ISM: kinematics and dynamics — stars: formation

1. INTRODUCTION

HH 80/81/80N is a spectacular and very luminous HH outflow spanning about 5 pc and exhibiting proper motions, close to the exciting source, of up to 1400 km s^{-1} (Reipurth & Graham 1988; Martí, Rodríguez, & Reipurth 1993, 1995, 1998; Heathcote, Reipurth, & Raga 1998; Molinari, Noriega-Crespo, & Spinoglio 2001). HH 80 North (hereafter HH 80N), the northern counterpart of HH 80/81, is optically invisible because of the high extinction at this position (Martí et al. 1993), but its radio and far-IR properties confirm its HH nature (Martí et al. 1993; Molinari et al. 2001). Far-IR *Infrared Space Observatory* observations show that the strong far-UV field radiated by the HH 80/81/80N outflow has induced the formation of a photodissociation region (PDR) in its immediately surrounding region (Molinari et al. 2001).

Molecular line observations toward HH 80N (Girart et al. 1994; Girart, Ho, & Estalella 1998) showed that it belongs to the class of Herbig-Haro (HH) objects, typically of high excitation, that are found to have starless quiescent dense clumps ahead of them. The strong radiation arising from the HH objects penetrates the clumps, releasing the icy mantles from the dust grains and inducing a photon-dominated chemistry, which causes significantly altered chemistry (Taylor & Williams 1996; Viti & Williams 1999). Recent observations toward HH 2 have confirmed this chemical scenario (J. M. Girart et al. 2001, in preparation). However, the presence of IRAS 18163−2042 associated with the HH 80N dense clump suggested that it could be tracing an embedded star (Girart et al. 1998).

This Letter presents CS and CO BIMA observations that are part of a molecular line survey toward HH 80N whose complete results will be reported in a forthcoming paper. The observations presented in this Letter show infall and outflow signatures associated with the dense clump downstream of HH 80N. The high angular resolution provided by millimeter interferometers, as in this Letter, have allowed astronomers to resolve spatially infall kinematical signatures in some low-mass star-forming cores (Zhou, Evans, & Wang 1996; Ohashi et al. 1997; Saito et al. 1996; Momose et al. 1998; Hogerheijde 2001). Typically, the infalling gas arises from scales of $\sim$1000–3000 AU, and the mass infall rates are (1–10) $\times$ 10^{-6} $M_\odot$ yr^{-1}. Interestingly, the infall signatures found in HH 80N are similar to that from the dense cores in L1544 (Ohashi et al. 1999) and HH 1/2 (Torrelles et al. 1994), which show infall signatures in the form of an almost ringlike structure in the position-velocity (PV) diagram on even larger scales, 1.5 $\times$ 10^4 and 4.5 $\times$ 10^4 AU, respectively.

2. OBSERVATIONS AND RESULTS

The observations were carried out between 1999 May and September with the 10-antenna BIMA array[5] at the Hat Creek Radio Observatory. The phase calibrator used was QSO 1733−130. The absolute flux calibration was performed by observing Uranus and Mars. The phase center of the observations was α(J2000) = 18^{h}19^{m}18^s.62, δ(J2000) = −20°40′55″. Two different frequency setups were used in order to observe the CS J = 2–1 and CO J = 1–0 lines, which provided a spectral resolution of 0.3 and 0.5 km s^{-1}, respectively. Maps were made with the (u, v)-data weighted by the associated system temperatures.

2.1. *The* CS J = 2–1 *Emission*

The CS emission arises from an elongated structure in the northwest-to-southeast direction (with a position angle [P.A.] of $\sim$125°) consisting of two well-differentiated structures morphologically and kinematically (see Figs. 1 and 2): (1) The main core is centered at the position of the ammonia core (Girart et al. 1994). The PV plot along the major axis of the CS emission shows a ringlike structure, roughly symmetrical

[1] Departament d'Astronomia i Meteorologia, Universitat de Barcelona, Av. Diagonal 647, E-08028 Barcelona, Catalunya, Spain; jgirart@am.ub.es.

[2] Department of Astronomy, University of Illinois at Champaign-Urbana, 1002 West Green Street, Urbana, IL 61801.

[3] Department of Physics and Astronomy, University College London, Gower Street, London WC1E 6BT, England.

[4] Harvard-Smithsonian Center for Astrophysics, 60 Garden Street, Cambridge, MA 02138.

[5] The BIMA array is operated by the Berkeley-Illinois-Maryland Association with support from the National Science Foundation.

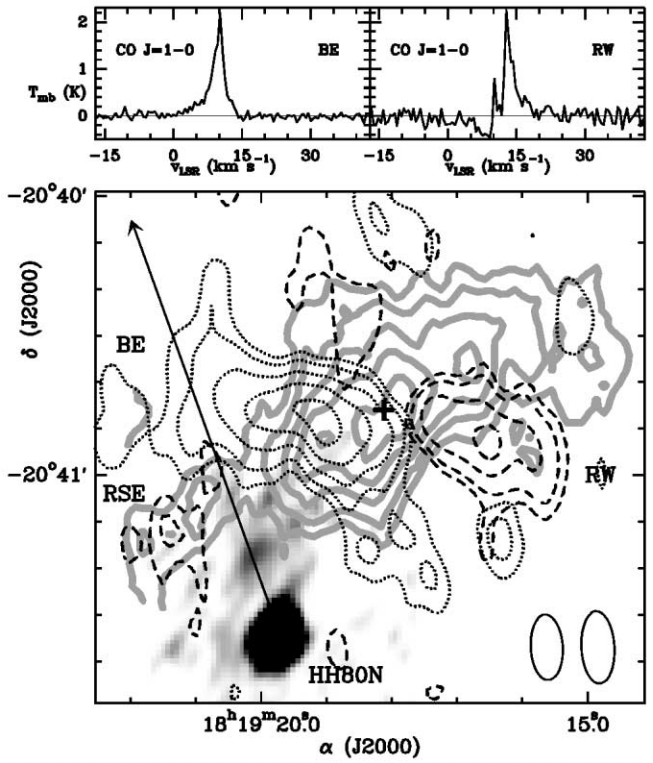

FIG. 1.—Superposition of the gray-scale map of the VLA 6 cm continuum emission from Martí et al. (1993), the thick gray contour map of the CS $J = 2$–1 integrated emission over the 9.8–13.6 km s^{-1} v_{LSR} interval, the thin dotted contour map of the averaged CO $J = 1$–0 blueshifted emission over the 4.7–9.7 km s^{-1} v_{LSR} interval, and the thin dashed contour map of the averaged CO $J = 1$–0 redshifted emission over the 12.7–17.7 km s^{-1} v_{LSR} interval. CS contours are 0.5, 1.0, 1.7, 2.4, and 3.1 Jy beam^{-1} km s^{-1}. CO contours are 3, 5, 8, 7, and 11 × 0.14 Jy beam^{-1}, the noise level of the maps. The cross indicates the position of the ammonia peak intensity (Girart et al. 1994). The solid arrow line shows the direction of the HH 80/81/80N flow. The half-power contour of the CS and CO synthesized beams (15″.6 × 7″.1, P.A. = 3° and 14″.9 × 8″.0, P.A. = 3°, respectively) are shown in the bottom left-hand corner, with the CS beam to the right. The top two panels show the CO $J = 1$–0 spectra averaged over the BE and RW lobes.

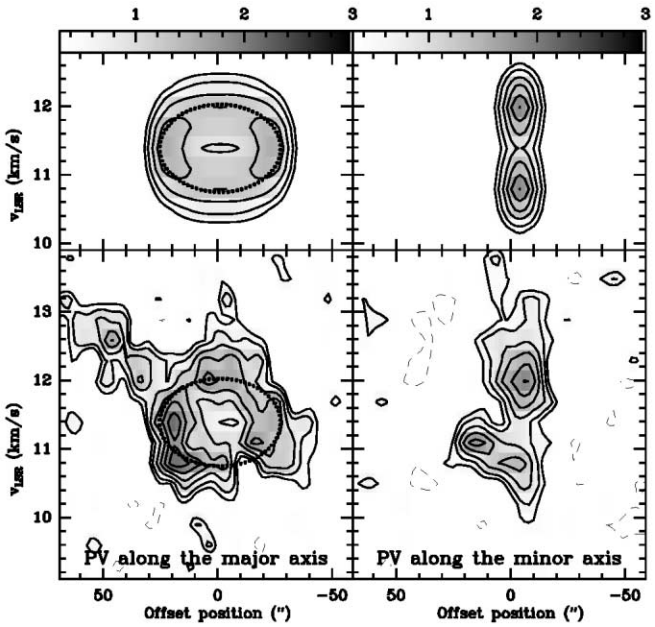

FIG. 2.—*Bottom left panel:* PV plot of CS $J = 2$–1 emission along the major axis of the dense core, P.A. = 125°, with the position offset relative to α(J2000) = 18^{h}19^{m}18^s.13, δ(J2000) = −20°40′40″.4. *Bottom right panel:* PV plot of CS $J = 2$–1 emission along the minor axis of the dense core. *Top panels:* Synthetic emission of the PV plots along the major (*left*) and minor (*right*) axis of an infalling ring with an infall velocity of 0.59 km s^{-1}, no rotation, an inner and outer radius of 0.19 and 0.29 pc, respectively, and a line width of 0.8 km s^{-1}.

about $V_{LSR} \simeq 11.4$ km s^{-1}. This structure can be explained by inward (or outward) motions in the condensation (see § 3.1) and resembles that from the starless core L1544 (Ohashi et al. 1999). The physical scale of the dense main core traced by the CS emission, ~0.48 × 0.17 pc (assuming a distance of 1.7 kpc; Martí et al. 1993), is larger than that from NH_3 (1, 1) (Girart et al. 1994) and HCO^+ $J = 3$–2 (Girart et al. 1998). This could be due to the higher critical density of these two lines with respect to the CS $J = 2$–1 transition. (2) A small redshifted "arm" (hereafter the RSE arm) is located southeast of the main core and ~15″ north of the 6 cm continuum emission. The RSE arm exhibits a clear linear velocity gradient with increasing velocity toward the east, i.e., as it gets closer to HH 80N. Table 1 shows the physical parameters of the core traced by the CS $J = 2$–1 line. Of the total mass measured [12 $M_\odot$, assuming X(CS) = 2 × 10^{-9}], around 10 $M_\odot$ belong to the main core, and 2 $M_\odot$ to the RSE arm.

2.2. *The Molecular Outflow*

The blueshifted and redshifted CO emission traces a clearly bipolar outflow along the east-west direction (lobes BE and RW) and approximately centered at the peak intensity of the CS-integrated emission (Fig. 1). The presence of molecular outflows is a clear signpost of star formation within the dense core. The outflow axis is not perpendicular to the major axis of the main core. However, our angular resolution traces scales (~2 × 10^4 AU) much larger than the scales at which the collimation process occurs, ~1 AU (Shu et al. 1995). Table 1 shows the physical parameters of the molecular outflow. There is marginal evidence of another bipolar outflow in the north-

TABLE 1
PHYSICAL PARAMETERS OF THE HH 80N REGION[a]

Parameter	Value
Molecular Dense Core	
M ($M_\odot$)	$12(X/2 \times 10^{-9})^{-1}$
V_{core} (km s^{-1})	11.43[b]
ΔV_{core} (km s^{-1})	0.7[b]
R_{inn} (pc)	0.19[b]
R_{out} (pc)	0.29[b]
V_{rot} (km s^{-1})	≲0.20[b]
V_{infall} (km s^{-1})	0.59[b]
$\dot{P}_{infall}$ ($M_\odot$ km s^{-1} yr^{-1})	2 × 10^{-5}
$\dot{M}_{infall}$ ($M_\odot$ yr^{-1})	3 × 10^{-5}
Molecular Outflow	
M ($M_\odot$)	0.11
R_{max} (pc)	~0.4
V_{max} (km s^{-1})	10
τ_d (yr)	3.6 × 10^4
P ($M_\odot$ km s^{-1})	0.35
$\dot{P}$ ($M_\odot$ km s^{-1} yr^{-1})	1.0 × 10^{-5}
L_{mech} ($L_\odot$)	1.1 × 10^{-3}

[a] Assuming optically thin emission, LTE, and no correction for inclination of the outflow.
[b] From the infalling ring model (see § 3.1).

south direction and also centered in the dense core. In addition to the molecular outflow, there is a redshifted clump that coincides not only spatially with the RSE arm but also kinematically, suggesting that this CO emission traces the same gas as the CS at this location.

3. DISCUSSION

3.1. *The Collapse of the Main Core*

The PV plot along the major and the minor axes of the CS emission (Fig. 2) clearly suggests that the gas is either collapsing or expanding radially and that the emission arises from a ringlike or toroidal structure. A similar structure has being observed toward the starless core L1554 from CCS observations (Ohashi et al. 1999). The ratio between the major and minor axes of the CS emission gives an inclination angle of $\gtrsim 70°$. As pointed out by Ohashi et al. (1999), the fact that the emission is detected toward a ringlike structure is probably due to a chemical effect, i.e., a decrease of the CS abundance toward the center, possibly because of gas depletion onto grains at higher densities (Rawlings et al. 1992).

We considered a model of a spatially thin ring with both infall and rotation, similar to that of Ohashi et al. (1997, 1999), seen edge-on by the observer. The parameters of the model were the inner and outer radii of the ring, $R_{\rm inn}$ and $R_{\rm out}$, the infall and rotation velocities, $V_{\rm infall}$ and $V_{\rm rot}$, and the intrinsic line width $\Delta V_{\rm core}$. The PV diagram was computed along the projected major and minor axes of the ring, assuming that the intensity was constant for $R_{\rm inn} < R < R_{\rm out}$, to compare with the observed kinematics. The best fit was obtained for velocities $V_{\rm infall} = 0.59$ km s^{-1}, $V_{\rm rot} \lesssim 0.20$ km s^{-1} and radii of the ring $R_{\rm inn} = 0.19$ pc, $R_{\rm out} = 0.29$ pc (see Table 1). The observed and synthetic PV diagrams are shown in Figure 2. This model also applies if the ring is expanding instead of contracting. In this case, the derived infall velocity should be taken as the expansion velocity.

Can the protostellar wind cause the expansion of a ringlike structure? The momentum rate of the ring (see Table 1) is $\sim 2 \times 10^{-5}\ M_\odot$ km s^{-1} yr^{-1}. On the other hand, the momentum rate of the protostellar wind, assuming that it is the same as that from the molecular outflow, is $\sim 1 \times 10^{-5}\ M_\odot$ km s^{-1} yr^{-1}. Although both values are similar, only a small fraction of the wind momentum rate would be transferred to the dense core. First, the dense core, as traced by the CS, shows a relatively flattened structure. Assuming that the ring structure traced by the CS is a torus, then the inner and outer radii derived from the model will imply a semiaperture angle of the torus as seen from the center of 12°. Second, the momentum rate distribution of the wind is expected to be anisotropic; i.e., most of the momentum rate of the wind is carried out along the axis of the outflow (e.g., Shu et al. 2000). The X-wind model (Shu et al. 1995) predicts that at a distance of 0.24 pc, the fraction of wind mass moving at equatorial angles lower than 12° is about 2% of the total wind mass. We expect the momentum rate to scale similarly. Thus, the wind that could interact with the dense core has a momentum rate of roughly 2×10^{-7} $M_\odot$ km s^{-1} yr^{-1}, which is much lower than that measured from the CS kinematics, assuming a typical CS abundance of $X({\rm CS}) = 2 \times 10^{-9}$. Thus, the wind would be able to cause the expansion of the ring only if the CS has an unusually high abundance, and if the true momentum rate is much higher than that measured, because of the outflow inclination and the optical depth.

Can the ringlike structure be in contraction? Girart et al. (1994) found that the ammonia emission arises from a smaller region than CS $J = 2$–1 and traces a 20 $M_\odot$ core (see § 2). This mass is similar to that required to cause free-fall collapse for the infall velocity measured at a radius of ~0.24 pc. However, the gas pressure and magnetic field should be taken into account. For the intrinsic line width obtained from the model, the virial mass without magnetic field for the CS main core is 9 $M_\odot$. This indicates that in the absence of the magnetic field, the gas pressure cannot prevent the collapse. Assuming that the ringlike structure is contracting, we can provide a rough upper limit on $|\boldsymbol{B}|$; i.e., the main core should be supercritical, and the total virial mass (including the magnetic fields) should be no more than the free-fall mass. Following the formulae given by Crutcher (1999) and McKee et al. (1993), we find that for a mass of 20 $M_\odot$, the collapse is possible for $|\boldsymbol{B}| < 50$ μG. Magnetic fields of $\lesssim 50$ μG have been measured in several molecular clouds with similar sizes and line widths as those of HH 80N (Crutcher 1999). Thus, it seems that there is enough mass to cause collapse while, on the other hand, an expansion would require an unusually high CS abundance and a high correction to the observed CO momentum rate. Therefore, we favor that the CS kinematics is tracing infall.

Compared with most of the low-mass regions where a kinematical infall signature has been found (see § 1), the HH 80N main core has a larger mass infall rate (see Table 1). This is probably because it is also a more massive region. Another example is the infalling NH_3 core in HH 1/2 (Torrelles et al. 1994), where the infall material also comes from a ringlike structure (toroid) with a similar size and mass as the HH 80N main core. Interestingly, the HH 80N and HH 1/2 star-forming cores show clear differences from the other collapsing ringlike structures detected so far. Here the infalling motions are clearly supersonic, with no rotation observed, whereas the infall motions in the starless core L1544 are subsonic and on the order of the rotation speeds (Tafalla et al. 1998; Ohashi et al. 1999; Williams et al. 1999). These differences could be due to an evolutionary effect (L1544 is still a starless core) and/or to the different masses involved in the collapse. The powering source of HH 1/2 is a protostar with an far-IR luminosity of ~50 $L_\odot$ (Harvey et al. 1986), but what about HH 80N?

3.2. *The Evolutionary Stage of the HH 80N Main Core*

IRAS 18163−2042 has a luminosity of ~20 $L_\odot$ (Girart et al. 1994), but because of the large position uncertainty it is possible that both the PDR region heated by HH 80N (Molinari et al. 2001) and the protostar embedded in the infalling core contribute to this luminosity, Therefore, this value is a rough upper limit of the protostellar luminosity.

A detailed study of the outflow activity, from a homogeneous sample of low-luminosity embedded young stellar objects (YSOs), done by Bontemps et al. (1996) found that the relation between the outflow momentum flux, the envelope mass, and the bolometric luminosity depends on the evolutionary stage of the protostars. In particular, the relation between $F_{\rm CO}c/L_{\rm bol}$ and $M_{\rm env}/L_{\rm bol}^{0.6}$, which should be almost free of any distance and luminosity effects, is useful to distinguish the evolutionary stage of the low-mass YSOs, i.e., whether they are in the Class 0 or I stage. The values of the measured envelope mass and the corrected momentum rate, $F_{\rm CO} = 10\dot{P}$ (the same inclination and opacity correction factor used by Bontemps et al. 1996), suggest that for the possible range of bolometric luminosities ($\lesssim 20\ L_\odot$), the HH 80N dense core is in the Class 0 evolutionary stage. Bontemps et al. (1996) also found that the momentum

flux and the envelope mass are well correlated for both Class 0 and I objects. However, taking into account the momentum flux of the HH 80N molecular outflow, the dense core is an order of magnitude more massive than what is expected from this correlation. The excess of envelope mass with respect to the outflow strength could be explained if there is multiple star formation going on (e.g., if at unresolved scales the core splits into several clumps, with some of them still prestellar).

3.3. *Interaction between HH 80N and the Molecular Cloud*

There are two observational features that suggest that the HH80/81/80N outflow may be interacting with the ambient gas surrounding the infalling main core: (1) the clear velocity gradient of the RSE arm is seen in both CS and CO emission, and its location is just above HH 80N (see Fig. 2), and (2) the BE lobe of the molecular outflow spreads out to the north at the position where it coincides spatially with the axis of the HH80/81/80N outflow (see Fig. 1; the arrow line indicates the outflow direction of HH 80N). This scenario, in which HH 80N and the dense gas are almost cospatial, suggests that the infalling dense core and the RSE arm may still be affected chemically by the strong UV radiation of HH 80N, as suggested by Girart et al. (1994, 1998), since this radiation is so strong that it has created a PDR region in its closest vicinity (Molinari et al. 2001).

It is unlikely that HH 80N triggered the star formation within the main core: assuming a HH 80N propagation speed of 100–300 km s^{-1} and using the typical age of a Class 0 source for the YSO embedded in the main core, $\sim 10^4$ yr, HH 80N would have had to be about 1–3 pc away from the main core when the collapse was initiated. Yet the material from the HH80/81/80N flow was likely present near to the CS core before HH 80N arrived to its proximity: a giant bow shock is observed downstream of HH80/81 (Heathcote et al. 1998), and the analysis of the line emission from HH80/81/80N shows that the shocks arise at the interface between two fast-moving flows (Molinari et al. 2001). Therefore, it is still possible that the HH80/81/80N outflow has triggered or at least sped up the star formation. There are many uncertainties in our understanding of the dynamics of collapse; these dynamics are determined by the balance of gravity against pressure. Once the collapse is triggered, it is not yet clear how infall proceeds since thermal and nonthermal pressure may support the clump from collapsing or at least retard an, often assumed, free-fall collapse (Rawlings et al. 1992). In the case of HH 80N, the UV radiation from the shock front may play an important role in the dynamics of the collapse of the dense core since it will highly affect its cooling function. Viti & Williams (1999) showed that the radiation generated in the HH shock drives a rapid chemistry in the dense core, by lifting the icy mantles and therefore enhancing the gas with hydrogenated species, such as NH_3 and H_2O; the latter, for example, will undoubtedly cool the gas. This would "encourage" the infall. This scenario will be investigated in a future paper.

We would like to thank Jorge Cantó, Frank Shu, and the anonymous referee for their valuable comments. J. M. G. is supported by NSF grant AST 99-81363 and by RED-2000 from the Generalitat de Catalunya. R. E. is partially supported by DGICYT grant PB98-0670 (Spain). S. V. and D. A. W. thank PPARC for supporting their research.

REFERENCES

Bontemps, S., Andre, P., Terebey, S., & Cabrit, S. 1996, A&A, 311, 858
Crutcher, R. M. 1999, ApJ, 520, 706
Girart, J. M., Estalella, R., & Ho, P. T. P. 1998, ApJ, 495, L59
Girart, J. M., et al. 1994, ApJ, 435, L145
Harvey, P. M., Joy, M., Lester, D. F., & Wilking, B. A. 1986, ApJ, 301, 346
Heathcote, S., Reipurth, B., & Raga, A. 1998, AJ, 116, 1940
Hogerheijde, M. R. 2001, ApJ, 553, 618
Martí, J., Rodríguez, L. F., & Reipurth, B. 1993, ApJ, 416, 208
———. 1995, ApJ, 449, 184
———. 1998, ApJ, 502, 337
McKee, C. F., Zweibel, E. G., Goodman, A. A., & Heiles, C. 1993, Protostars and Planets III, ed. E. H. Levy & J. I. Lunine (Tucson: Univ. Arizona Press), 327
Molinari, S., Noriega-Crespo, A., & Spinoglio, L. 2001, ApJ, 547, 292
Momose, M., Ohashi, N., Kawabe, R., Nakano, T., & Hayashi, M. 1998, ApJ, 504, 314
Ohashi, N., Hayashi, M., Ho, P. T. P., & Momose, M. 1997, ApJ, 475, 211
Ohashi, N., Lee, S. W., Wilner, D. J., & Hayashi, M. 1999, ApJ, 518, L41
Rawlings, J. M. C., Hartquist, T. W., Menten, K. M., & Williams, D. A. 1992, MNRAS, 255, 471
Reipurth, B., & Graham, J. A. 1988, A&A, 202, 219
Saito, M., Kawabe, R., Kitamura, Y., & Sunada, K. 1996, ApJ, 473, 464
Shu, F. H., Najita, J., Ostriker, E. C., & Shang, H. 1995, ApJ, 455, L155
Shu, F. H., Najita, J. R., Shang, H., & Li, Z.-Y. 2000, Protostars and Planets IV, ed. V. Mannings, A. Boss, & S. S. Russell (San Diego: Academic), 789
Tafalla, M., Mardones, D., Myers, P. C., Caselli, P., Bachiller, R., & Benson, P. J. 1998, ApJ, 504, 900
Taylor, S. D., & Williams, D. A. 1996, MNRAS, 282, 1343
Torrelles, J. M., Gómez, J. F., Ho, P. T. P., Rodríguez, L. F., Anglada, G., & Cantó, J. 1994, ApJ, 435, 290
Viti, S., & Williams, D. A. 1999, MNRAS, 310, 517
Williams, J. P., Myers, P. C., Wilner, D. J., & di Francesco, J. 1999, ApJ, 513, L61
Zhou, S., Evans, N. J., & Wang, Y. 1996, ApJ, 466, 296